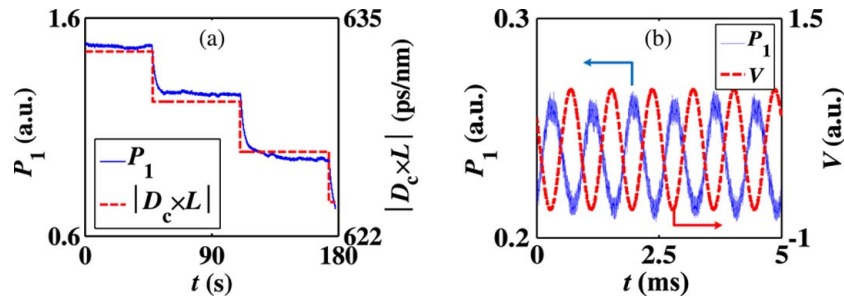


# Chromatic-Dispersion Monitor Based on a Differential Phase-Shift Method Using a Kerr Phase-Interrogator

Volume 7, Number 2, April 2015

Yang Lu  
Chams Baker  
Liang Chen  
Xiaoyi Bao



---

DOI: 10.1109/JPHOT.2015.2418259  
1943-0655 © 2015 IEEE

# Chromatic-Dispersion Monitor Based on a Differential Phase-Shift Method Using a Kerr Phase-Interrogator

Yang Lu, Chams Baker, Liang Chen, and Xiaoyi Bao

Department of Physics, University of Ottawa, Ottawa, ON K1N 6N5, Canada

DOI: 10.1109/JPHOT.2015.2418259

1943-0655 © 2015 IEEE. Translations and content mining are permitted for academic research only.

Personal use is also permitted, but republication/redistribution requires IEEE permission.

See [http://www.ieee.org/publications\\_standards/publications/rights/index.html](http://www.ieee.org/publications_standards/publications/rights/index.html) for more information.

Manuscript received December 15, 2014; revised March 25, 2015; accepted March 27, 2015. Date of publication March 31, 2015; date of current version April 15, 2015. This work was supported by the Natural Science and Engineering Research Council Discovery Grant and the Canada Research Chair Program (CRC in Fiber Optics and Photonics). The work of Y. Lu was supported by China Scholarship Council. Corresponding author: C. Baker (e-mail: cbake2@uottawa.ca).

**Abstract:** We present a novel approach for real-time chromatic-dispersion (CD) monitoring using a Kerr phase-interrogator. CD induces a differential phase shift between two sinusoidal signals carried by two different wavelengths. A Kerr phase-interrogator converts the differential phase shift into power variation, and CD monitoring is achieved by measurement of the power variation in real time. A CD monitor with a resolution of 0.196 ps/nm is experimentally demonstrated. The high sensitivity and fast response of this CD monitoring approach opens the way for novel sensing applications.

**Index Terms:** Nonlinear, Kerr effect, fiber non-linear optics, microwave photonics, microwave photonics signal processing.

## 1. Introduction

Real-time chromatic-dispersion (CD) monitoring is practical for automated CD compensation in high bit-rate and long-distance optical transmission systems [1]. Due to temperature and strain dependence of CD in optical fibers and chirped fiber Bragg gratings [2]–[5], CD monitors can be used for sensing applications. CD monitoring has been achieved using asynchronous amplitude sampling techniques and histogram evaluation approaches [6]–[8] where CD is acquired from statistical properties of the monitored optical signal. Time-consuming signal processing makes these statistical approaches impractical for real-time monitoring. Signal-modulation based approaches have also been used for monitoring CD by measurement of the peak-to-peak values of the amplitude modulated (AM) pilot tones [9]–[11], or the phase difference between the upper and lower sidebands of the AM pilot tones [12]. Signal-modulation approaches require broad-band detector to obtain the AM pilot tones and special electronic circuits such as phase-locked loops for signal processing, leading to complex signal acquisition and bandwidth limitations.

We have recently demonstrated a Kerr phase-interrogator that measures phase-shift between two sinusoidal signals carried by the same laser wavelength using phase-modulation induced by the Kerr effect [13]–[17]. The Kerr phase-interrogator can also measure the phase-shift between sinusoidal signals carried by different laser wavelengths, allowing for differential phase-shift measurement. Because the differential phase-shift is linearly proportional to the CD in the

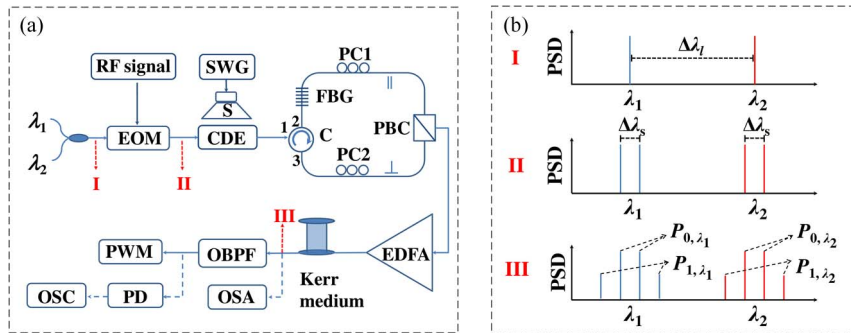


Fig. 1. (a) Schematic of the chromatic dispersion monitoring setup based on a Kerr phase-interrogator. (b) Illustrations of the optical spectra at different points of the setup. EOM: electro-optic modulator; RF: radio frequency; CDE: chromatic-dispersion emulator; SWG: sinusoidal waveform generator; S: speaker; C: circulator; FBG: fiber Bragg grating; PC: polarization controller; PBC: polarization beam combiner; EDFA: erbium-doped fiber amplifier; OBPF: optical band-pass filter; OSA: optical spectrum analyzer; PWM: power meter; PD: photodiode; OSC: oscilloscope; PSD: power spectral density.

propagation path of the two sinusoidal signals, the Kerr phase-interrogator can monitor CD variations allowing for novel sensing applications. In comparison with existing approaches, CD monitoring is achieved by a mere power measurement at the output of the Kerr phase-interrogator without additional signal-processing allowing for measurement of fast CD variations and, consequently, real-time CD monitoring.

In this paper, we propose and experimentally demonstrate a novel approach for real-time CD monitoring by a differential phase-shift method using a Kerr phase-interrogator. A Kerr phase-interrogator setup is configured for real-time CD monitoring by utilization of two orthogonally-polarized sinusoidal optical signals that are carried by two different laser wavelengths. Phase-modulation induced by the Kerr effect on the sinusoidal optical signals is theoretically analyzed showing that the power of the generated first-order sideband varies sinusoidally with CD. Real-time CD monitoring by measurement of the power of the first-order sideband is experimentally demonstrated.

## 2. Experimental Setup

Fig. 1(a) shows the Kerr phase-interrogator configured for CD monitoring. Two continuous-wave lasers (Agilent 81980A) operating at wavelengths  $\lambda_1$  and  $\lambda_2$  are amplitude-modulated by an electro-optic modulator (EO-Space) and a sinusoidal electrical signal generator (HP 83752A) at a radio frequency (RF)  $f_m$ . The outputs of the modulator are two sinusoidal optical signals oscillating at a frequency  $f_s = 2f_m$ . The optical spectrum for each sinusoidal optical signal consists of two distinct peaks separated by  $\Delta\lambda_s = (\lambda_1^2/c)f_s \approx (\lambda_2^2/c)f_s$  with  $c$  being speed of light in vacuum, as illustrated in Fig. 1(b). The modulated signals then propagate through a tunable CD emulator (TDC-109181917) that induces an accumulated CD equivalent to  $D_c \times L = t_d/\Delta\lambda_l$ , where  $D_c$  is the CD parameter;  $L$  is the propagation distance;  $t_d = t_2 - t_1$  is the group delay difference of two sinusoidal signals induced by CD emulator, with  $t_j$  being the group-delay accumulated by the sinusoidal signal carried by the laser carrier at  $\lambda_j$ ; and  $\Delta\lambda_l = \lambda_2 - \lambda_1$  is the laser carrier separation. The sinusoidal optical signals are separated using a fiber Bragg grating and a circulator, and then recombined using a fiber-coupled polarization beam combiner to obtain two orthogonally polarized sinusoidal optical signals. Two polarization controllers, i.e., PC1 and PC2, ensure the powers of the parallel and perpendicular components of the combined signal are maximum and equal. The combined signal is amplified by an Erbium-doped fiber amplifier (Amorphics AEDFA-33-B-FA) and then launched into a Kerr medium composed of a dispersion-shifted fiber (DSF) with a zero dispersion wavelength at  $\lambda = 1552$  nm, a length  $L_{Kerr} = 2.27$  km and waveguide nonlinearity  $\gamma = 2.28$  W<sup>-1</sup>/km.

The amplitude of the sinusoidal optical signal carried by  $\lambda_j$  at the input of the Kerr medium is given by

$$A_j = \sqrt{\frac{P_p}{2}} \cos[\pi f_s(t - t_j)] \quad (1)$$

where  $P_p$  is the total peak power of the combined signal. Neglecting CD effects in the Kerr medium, the evolution of the sinusoidal optical signals in a non-birefringent fiber is governed by the coupled nonlinear Schrodinger equations [18]

$$\frac{dA_{1m}}{dz} = i\gamma_1 (|A_{1m}|^2 + 2|A_{2m}|^2 + |A_{1n}|^2 + |A_{2n}|^2) A_{1m} \quad (2)$$

$$\frac{dA_{2n}}{dz} = i\gamma_2 (|A_{2n}|^2 + 2|A_{1n}|^2 + |A_{2m}|^2 + |A_{1m}|^2) A_{2n} \quad (3)$$

where  $\gamma_j$  is the waveguide nonlinearity at  $\lambda_j$ ,  $m = x, y$  and  $n = x, y$  with  $m \neq n$ ,  $x$  and  $y$  represent two orthogonal polarization states. Setting  $A_{1y} = A_{2x} = 0$  and  $\gamma_1 = \gamma_2 = \gamma$  leads to  $A_{1x} = A_1$ ,  $A_{2y} = A_2$ , and (2) and (3) reduce to

$$\frac{dA_j}{dz} = i\gamma (|A_1|^2 + |A_2|^2) A_j \quad (4)$$

with  $j = 1, 2$ , which has a solution  $A_j(L_{Kerr}) = A_j(0)\exp(i\phi_{NL})$ , where

$$\phi_{NL} = \frac{P_p \gamma L_{Kerr}}{2} \{ \cos^2[\pi f_s(t - t_1)] + \cos^2[\pi f_s(t - t_2)] \}. \quad (5)$$

The phase modulation induced by  $\phi_{NL}$  leads to the formation of distinct sidebands  $P_k$  with  $k = 1, 2$ , [13], [14], as illustrated in Fig. 1(b). The ratio of  $P_1$  to  $P_0$  is derived analytically as described in [14] to obtain

$$\frac{P_1}{P_0} = \frac{J_1^2 \left[ \frac{\phi_{SPM}}{2} \cos(\phi) \right] + J_2^2 \left[ \frac{\phi_{SPM}}{2} \cos(\phi) \right] \pm 2\sin(\phi) J_1 \left[ \frac{\phi_{SPM}}{2} \cos(\phi) \right] J_2 \left[ \frac{\phi_{SPM}}{2} \cos(\phi) \right]}{J_0^2 \left[ \frac{\phi_{SPM}}{2} \cos(\phi) \right] + J_1^2 \left[ \frac{\phi_{SPM}}{2} \cos(\phi) \right] \pm 2\sin(\phi) J_0 \left[ \frac{\phi_{SPM}}{2} \cos(\phi) \right] J_1 \left[ \frac{\phi_{SPM}}{2} \cos(\phi) \right]} \quad (6)$$

where the positive and negative signs refer to  $A_1$  and  $A_2$ , respectively,  $\phi_{SPM} = P_p \gamma L_{Kerr}$ ,  $\phi = \pi f_s t_d + \phi_0$  with  $\phi_0$  being a constant, and  $t_d = D_c \Delta \lambda_l L$ . For  $\phi_{SPM} < 0.5$ , (6) reduces to

$$P_1 = P_1^{max} \cos^2(\pi f_s D_c \Delta \lambda_l L + \phi_0) \quad (7)$$

where  $P_1^{max}$  is the maximum value of  $P_1$  [14].

### 3. Experimental Results

The operating wavelengths of the lasers are set to  $\lambda_1 = 1550.05$  nm and  $\lambda_2 = 1550.91$  nm, and the modulation frequency is set to  $f_m = 9$  GHz. The accumulated CD is varied from  $-617$  ps/nm to  $-641$  ps/nm in steps of 6 ps/nm and the spectrum of the signal at the output of the Kerr medium is measured by an optical spectrum analyzer (Yokogawa AQ6370C). Fig. 2(a) presents the evolution of the measured spectra at the output of Kerr medium as the accumulated CD is varied and Fig. 2(b) presents a magnified image of the generated first-order sideband. The first-order sideband is extracted by a band-pass filter (TeraXion TFC) with a 3 dB bandwidth of 3 GHz, and a power meter (Agilent/HP 81536A) is used to measure  $P_1$  as the accumulated CD is varied. Fig. 2(c) presents the measured values of normalized power  $P_1/P_1^{max}$  as the accumulated CD is varied between  $-644$  ps/nm and  $-584$  ps/nm, in steps of 3 ps/nm. The normalized power calculated using (7), showing close agreement with experimental values, is also presented in Fig. 2(c).

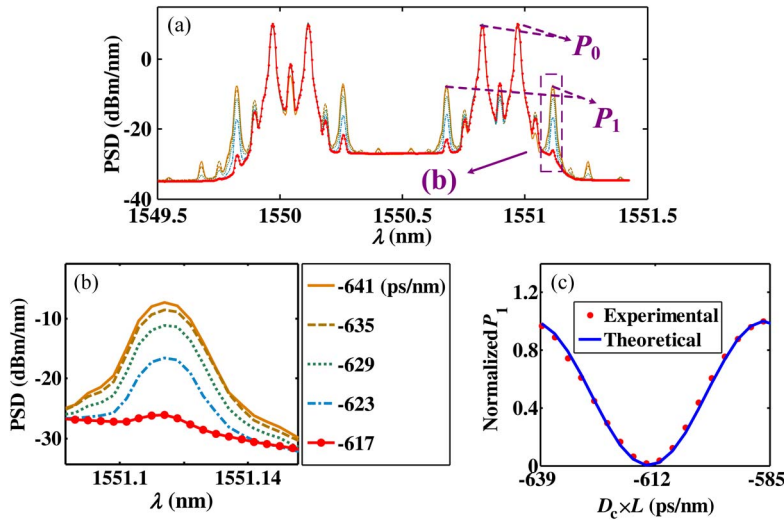


Fig. 2. (a) Measured spectra at the output of the Kerr medium and (b) a magnified image of the first-order sideband. (c) Experimentally measured and theoretically calculated values of normalized power  $P_1/P_1^{\max}$  as a function of the accumulated CD.

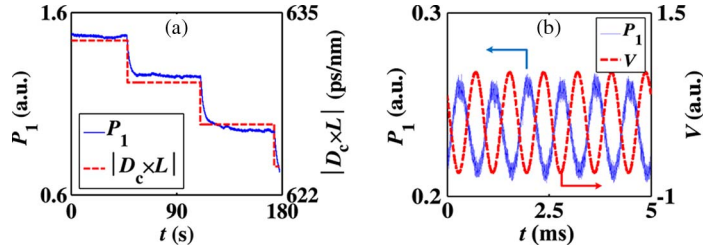


Fig. 3. (a) Measured trace of  $P_1$  as a function of time as  $|D_c \times L|$  decreases in steps of 3 ps/nm every minute. (b) Measured trace of  $P_1$  as a function of time showing the vibration induced variation in  $|D_c \times L|$ .

The power-meter is replaced by a photodiode that is connected to an electrical oscilloscope (Agilent DSO81204B) to record the real-time value of  $P_1$  as the accumulated CD is varied. The accumulated CD is varied by a step of 3 ps/nm every minute in the range between  $-633$  ps/nm and  $-624$  ps/nm where  $P_1$  has quasi-linear dependence on the accumulated CD. Fig. 3(a) presents the measured trace of  $P_1$  as a function of time showing correspondence between  $P_1$  and the accumulated CD, as well as power fluctuation in the measured trace arises from the CD-fluctuation from the emulator.

A speaker is placed on top of the CD emulator and is driven with a sinusoidal waveform generator at a frequency of 1.2 kHz. The acoustic wave from the speaker induces mechanical vibrations in the chirped fiber Bragg grating of the CD emulator leading to periodic variation of the accumulated CD. Real-time variation of the accumulated CD is monitored by measurement of the sideband power  $P_1(t)$ . Fig. 3(b) presents the measured trace of  $P_1(t)$  with a trace of the voltage that is used to drive the speaker showing correlation between these two signals.

#### 4. Discussion

The resolution of proposed CD monitor is determined by the minimum resolvable differential phase-shift  $\alpha = \pi f_s D_c \Delta \lambda / L$ . Differentiation of (7) leads to  $|\delta \phi \sin(2\phi)| = |\delta P_1 / P_1^{\max}|$ , where  $\delta \phi$  and  $\delta P_1$  represent fluctuations of phase-shift and power, respectively. Around the quadrature points at  $\phi = \pi/4 + m\pi/2$  where  $m$  is an integer, the phase fluctuation is given by  $|\delta \phi| = |\delta P_1 / P_1^{\max}|$ . The minimum resolvable differential phase-shift  $\alpha = \max\{|\delta \phi|\}$  can be verified experimentally

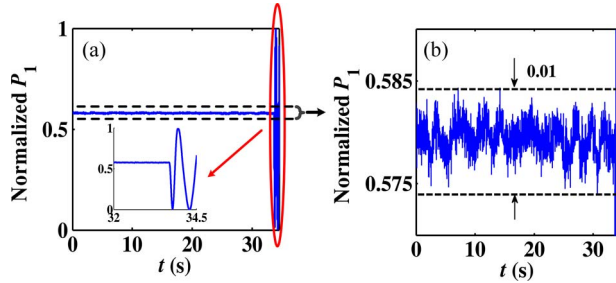


Fig. 4. (a) Measured trace of  $P_1/P_1^{\max}$  as a function of time with an inset showing the full power swing that results from changing  $|D_c \times L|$  by 100 ps/nm. (b) Magnified image showing the fluctuation of the normalized power when  $|D_c \times L|$  is unchanged.

from the power fluctuations  $|\delta P_1/P_1^{\max}|$ . Fig. 4(a) presents a measured trace of normalized  $P_1$  as a function of time where the accumulated CD is fixed at  $-628$  ps/nm over a duration of  $33$  s and then is changed abruptly by  $100$  ps/nm. Fig. 4(b) presents a magnified image of the measured trace showing that  $|\delta P_1/P_1^{\max}| < 0.01$  leading to  $\alpha = 0.01$  rad around quadrature points. Using  $f_s = 18$  GHz,  $\Delta\lambda_l = 0.9$  nm, and  $\alpha = 0.01$  rad leads to a CD monitor resolution of  $0.196$  ps/nm.

Fluctuations of  $P_1$  are induced by the noise in the peak power  $P_P$  of the combined sinusoidal optical signal at the input of the Kerr medium. The peak power noise arises from the intensity-noise of the laser and the amplified spontaneous-emission noise of the EDFA. Peak power noise also arises from external mechanical and thermal disturbances that cause birefringence variation in the monitored device which induce polarization variation on sinusoidal optical signals before PBC. The noise of  $P_P$  induces variations to  $\phi_{SPM} = P_P \gamma L_{Kerr}$  and  $P_0 \approx P_P/4$  which, according to (6), lead to fluctuations in the power of the first-order sideband  $\delta P_1$ . Shot-noise and dark-current noise of the photo-detector further increase the magnitude of  $\delta P_1$ . The resulting  $\delta P_1$  leads to phase fluctuations  $|\delta\phi| = |\delta P_1/P_1^{\max}|$ , which limit the minimum resolvable differential phase-shift  $\alpha$ , and consequently, limit the finesse of the achievable resolution. The magnitude of  $\delta P_1$  can be reduced by utilization of a laser with low intensity-noise, a highly nonlinear Kerr-medium to eliminate the need for the EDFA, and a low noise photo-detector. Furthermore, external disturbances that cause polarization variation are relatively slow and their contribution to  $\delta P_1$  can be eliminated by using a feedback control-system that corrects the polarization of the sinusoidal optical signals before the PBC.

The dynamic-range  $\{D_c \times L\}_{DR}$  is not limited by the equipment that comprise the CD monitor. In practice, a value of  $P_1$  corresponds to multiple values of the accumulated CD due to the sinusoidal variation of  $P_1$  with  $D_c \times L$ . To avoid post-measurement signal processing and obtain a one-to-one correspondence between  $P_1$  and  $D_c \times L$ , the dynamic-range  $\{D_c \times L\}_{DR}$  is restricted within the quasi-linear range over which  $P_1$  varies from  $0.2P_{\max}$  to  $0.8P_{\max}$  around the quadrature points [17]. Fig. 2(c) shows that  $P_1 = 0.2P_{\max}$  at  $D_c \times L = -621.0$  ps/nm and  $P_1 = 0.8P_{\max}$  at  $D_c \times L = -633.5$  ps/nm leading to  $\{D_c \times L\}_{DR} = 12.5$  ps/nm. The value of  $\{D_c \times L\}_{DR}$  is estimated from (7) to be  $\{D_c \times L\}_{DR} \approx 1/4f_s\Delta\lambda_l$ . Using  $f_s = 18$  GHz and  $\Delta\lambda_l = 0.9$  nm leads to  $\{D_c \times L\}_{DR} = 15.4$  ps/nm, which is in close agreement with the measured value.

Derivation of (7) utilizes the assumption that CD is negligible in the Kerr medium. This assumption is valid when the group-delay difference  $|\Delta t| = |D_{c,Kerr}|L_{Kerr}\Delta\lambda_l$  that is induced by the CD of the Kerr medium is negligible in comparison to the period of the sinusoidal optical signal  $T_s = 1/f_s$ . For our experiment, the CD parameter of the DSF that comprises the Kerr medium is  $D_{c,Kerr} \approx -0.04$  ps/nm-km at  $\lambda_1$  and  $\lambda_2$ , as measured in [16],  $L_{Kerr} = 2.27$  km, and  $\Delta\lambda_l = 0.9$  nm, leading to  $|\Delta t| = 0.082$  ps, which is much smaller than  $T_s = 55.56$  ps.

## 5. Conclusion

We present a novel approach for real-time CD monitoring by utilizing a Kerr phase-interrogator. CD induced group-delay difference of two sinusoidal optical signals carried by two different

wavelengths is converted to power variation by a Kerr phase-interrogator. Monitoring of CD at a resolution of 0.196 ps/nm is experimentally demonstrated. High-resolution real-time CD monitoring opens ways for novel sensing applications, as will be presented in future work.

## References

- [1] D. C. Kilper *et al.*, "Optical performance monitoring," *J. Lightw. Technol.*, vol. 22, no. 1, pp. 294–304, Jan. 2004.
- [2] W. H. Hatton and M. Nisimura, "Temperature dependence of chromatic dispersion in single mode fibers," *J. Lightw. Technol.*, vol. 4, no. 10, pp. 1552–1555, Oct. 1986.
- [3] M. E. Lines, "Physical origin of the temperature dependence of chromatic dispersion in fused silica," *J. Appl. Phys.*, vol. 73, no. 5, pp. 2075–2079, Mar. 1993.
- [4] T. Imai, T. Komukai, and M. Nakazawa, "Dispersion tuning of a linearly chirped fiber Bragg grating without a center wavelength shift by applying a strain gradient," *IEEE Photon. Technol. Lett.*, vol. 10, no. 6, pp. 845–847, Jun. 1998.
- [5] C. S. Goh, S. Y. Set, and K. Kikuchi, "Design and fabrication of a tunable dispersion-slope compensating module based on strain-chirped fiber Bragg gratings," *IEEE Photon. Technol. Lett.*, vol. 16, no. 2, pp. 524–526, Feb. 2004.
- [6] F. N. Khan, A. P. T. Lau, C. Lu, and P. K. A. Wai, "Chromatic dispersion monitoring for multiple modulation formats and data rates using sideband optical filtering and asynchronous amplitude sampling technique," *Opt. Exp.*, vol. 19, no. 2, pp. 1007–1015, Jan. 2011.
- [7] B. Kozicki, A. Maruta, and K. Kitayama, "Transparent performance monitoring of RZ-DQPSK systems employing delay-tap sampling," *J. Opt. Netw.*, vol. 6, no. 11, pp. 1257–1269, Nov. 2007.
- [8] Z. Li and G. Li, "Chromatic dispersion and polarization-mode dispersion monitoring for RZ-DPSK signals based on asynchronous amplitude-histogram evaluation," *J. Lightw. Technol.*, vol. 24, no. 7, pp. 2859–2866, Jul. 2006.
- [9] A. L. Campillo, "Chromatic dispersion-monitoring technique based on phase-sensitive detection," *IEEE Photon. Technol. Lett.*, vol. 17, no. 6, pp. 1241–1243, Jun. 2005.
- [10] M. N. Petersen, Z. Pan, S. Lee, S. A. Havstad, and A. E. Willner, "Online chromatic dispersion monitoring and compensation using a single inband subcarrier tone," *IEEE Photon. Technol. Lett.*, vol. 14, no. 4, pp. 570–572, Apr. 2002.
- [11] K. J. Park, J. H. Lee, C. J. Youn, and Y. C. Chung, "A simultaneous monitoring technique for polarization-mode dispersion and group-velocity dispersion," in *Proc. OFC*, 2002, pp. 199–200.
- [12] T. E. Dimmick, G. Rossi, and D. J. Blumenthal, "Optical dispersion monitoring technique using double sideband subcarriers," *IEEE Photon. Technol. Lett.*, vol. 12, no. 7, pp. 900–902, Jul. 2000.
- [13] M. Rochette, C. Baker, and R. Ahmad, "All-optical polarization-mode dispersion monitor for return-to-zero optical signals at 40 Gbits/s and beyond," *Opt. Lett.*, vol. 35, no. 21, pp. 3703–3705, Nov. 2010.
- [14] C. Baker and X. Bao, "Displacement sensor based on Kerr induced phase-modulation of orthogonally polarized sinusoidal optical signals," *Opt. Exp.*, vol. 22, no. 8, pp. 9095–9100, Apr. 2014.
- [15] C. Baker, Y. Lu, J. Song, and X. Bao, "Incoherent optical frequency domain reflectometry based on a Kerr phase-interrogator," *Opt. Exp.*, vol. 22, no. 13, pp. 15 370–15 375, Jun. 2014.
- [16] C. Baker, Y. Lu, and X. Bao, "Chromatic-dispersion measurement by modulation phase-shift method using a Kerr phase-interrogator," *Opt. Exp.*, vol. 22, no. 19, pp. 22 314–22 319, Sep. 2014.
- [17] Y. Lu, C. Baker, L. Chen, and X. Bao, "Group-delay based temperature sensing in linearly-chirped fiber Bragg gratings using a Kerr phase-interrogator," *J. Lightw. Technol.*, vol. 33, no. 2, pp. 381–385, Jan. 2015.
- [18] S. Kumar, A. Selvarajan, and G. V. Anand, "Nonlinear copropagation of two optical pulses of different frequencies in birefringent fibers," *J. Opt. Soc. Amer. B, Opt. Phys.*, vol. 11, no. 5, pp. 810–817, May 1994.